EARTHQUAKE ENGINEERING AND STRUCTURAL DYNAMICS
Earthquake Engng Struct. Dyn. 2000; **29**: 481–498

Investigation of dynamic cable–deck interaction in a physical model of a cable-stayed bridge. Part I: modal analysis

E. Caetano[1], A. Cunha[1]* and C. A. Taylor[2]

[1]*Faculty of Engineering, University of Porto, Rua dos Bragas, 4099 Porto Codex, Portugal*
[2]*Earthquake Engineering Research Centre, University of Bristol, Queen's Building, University Walk, Bristol BS8 1TR, UK*

SUMMARY

A description of an experimental investigation involving the study of the dynamic interaction between the cables and the deck/towers system in cable-stayed bridges is presented. The work was carried out on a physical model of a cable-stayed bridge (the Jindo Bridge, in South Korea), whose characteristics of stiffness and mass have been conveniently scaled. Standard modal analysis tests were performed using both an electrodynamic shaker and a shaking table, leading to the creation of a high-quality database, characterizing the dynamic behaviour of the bridge. The study shows the existence of a clear dynamic interaction between the cables and the deck/towers system, associated with the appearance of several groups of mode shapes, at closely spaced frequencies, involving different cable movements, but similar configurations of the girder and towers. Copyright © 2000 John Wiley & Sons, Ltd.

KEY WORDS: cable-stayed bridges; physical models; modal analysis; shaking table; cable dynamics

1. INTRODUCTION

The peculiarity of the structural behaviour of cable-stayed bridges, in particular under dynamic excitations (wind, earthquakes and traffic loads), naturally requires the adoption of sophisticated dynamic analysis procedures. Although there has been recently a significant effort to improve numerical formulations for the modelling of the structural behaviour, it is of great interest to perform experimental tests, both on prototypes and on physical models, to improve and validate the mathematical models, and to study some peculiar forms of behaviour not yet completely understood.

Some physical models have been tested in the past [1–3]. However, not all of them were replicas of specific prototypes. Only in a few cases were some correlations achieved between the analytical response of the prototype and the measured response of the model to some dynamic

* Correspondence to: A. Cunha, Faculty of Engineering, University of Porto, Rua dos Bragas, 4099 Porto Codex, Portugal.

Received 12 June 1997
Revised 27 May 1999
Accepted 28 September 1999

excitation. Full-scale vibration tests on cable-stayed bridges have also been reported in the literature, as it is the case of Annacis [4], Tjörn [5] or Tampico [6] bridges.

From these tests and from visual observation of other cable structures, some particular aspects associated with the dynamics of cable-stayed bridges have been identified, such as the occurrence of important stay cable oscillations, sometimes conjugated with simultaneous vibration of the deck. This phenomenon has been clearly evidenced by long-term monitoring of some modern bridges, namely Faroe [5], Helgeland [7], Ben-Ahin and Wandre [8] bridges. Although there is not yet a complete knowledge of the mechanism behind these cable oscillations, several possible causes have been considered [9], namely (i) excitation caused by vortex shedding from behind the pylons, the girder or the cables [10], (ii) direct excitation from the wind due to turbulent flow, (iii) excitation due to oscillation of the cable supports (parametric excitation) [11] and (iv) rain-induced vibration [12]. Each of these aspects has been the subject of recent investigations, in many cases accompanied by the development of laboratory tests on individual cables [13]. Considering these aspects in the study of the global behaviour of a cable-stayed bridge, some authors [5,14,15] have stressed the significance of modelling the distributed inertia of the cables in the numerical model of the bridge, so as to include the corresponding vibration modes in the dynamic analysis of the whole structure. However, to the authors' knowledge, the degree of importance of cable vibration in terms of the dynamic response of cable-stayed bridges has not yet been fully evaluated.

Using a numerical approach, Abdel-Ghaffar and Khalifa [15] emphasized the importance of complex vibrations of stay cables, which seem to be strongly coupled with the bridge deck and tower motions, although they are usually overlooked or treated independently in most studies of cable-stayed bridges. According to Abdel-Ghaffar and Khalifa, by discretizing each cable into small finite elements, there results new and numerous complex pure cable vibration modes, whose analytical prediction would be impossible using the linearized natural frequency expressions for the individual inclined cables. Furthermore, this model also provides coupled deck-cable motions involving bending and torsional motions of the deck, as well as vertical and swinging cable motions. These cannot be predicted using traditional finite element models, and may have a significant effect on the participation factors used in the earthquake response calculation.

The present paper describes some results of an investigation conducted at the Earthquake Engineering Research Centre of the University of Bristol (U.K.), in collaboration with the University of Porto (Portugal), with the aim of experimentally confirming the existence and importance of the interaction between the stay cables and the deck-towers system in a cable-stayed bridge. This study has been performed on the physical model of a cable-stayed bridge (the Jindo Bridge, in South Korea), whose characteristics of stiffness and mass have been conveniently scaled. Standard experimental modal analysis techniques have been employed in order to identify the main dynamic parameters of the bridge, using both an electrodynamic shaker and a shaking table. Various series of mode shapes were identified at very close frequencies, involving similar configurations of the girder and towers, but different cable movements. A comparison between experimental and numerical results was made.

In order to evaluate the importance of the dynamic cable–deck interaction in terms of the response to seismic excitations, several shaking table tests were also performed, considering different types of artificial accelerograms. Results of these tests, as well as of numerical simulations, are presented in a companion paper [16].

2. THE JINDO BRIDGE PROTOTYPE

The Jindo Bridge, designed by Rendel Palmer and Tritton and built in South Korea [17], is a three span steel cable-stayed bridge with a continuous stiffening girder, having a total length of 484 m. The main span is 344 m and the side spans are 70 m, according to the scheme of Figure 1. The boundary conditions of the main girder are achieved by two rocker supports at the ends, one pinned support at one of the towers and a roller at the other tower. The stays are arranged in a form of a fan converging at the top of each A-frame tower. Each tower carries 24 stays. The cables are locked coil ropes.

3. THE PHYSICAL MODEL OF JINDO BRIDGE

The physical model of Jindo Bridge, built at the Earthquake Engineering Research Centre of the University of Bristol, can be described as a distorted small-scale model with artificial mass simulation. This model was designed by Garevski [3], who performed damping and seismic response measurement tests, and was slightly modified by the authors [18], in order to study appropriately the problem of coupled cable–deck motions.

The model satisfied similarity for the bending stiffness of the girder and towers and for the axial stiffness of the cable stays. The design of new additional masses for the cables attempted to simulate correctly their continuous mass distribution while using an efficient form of fixation. A complete description of this design process, based on the similarity theory, was previously reported by the authors in Reference (18).

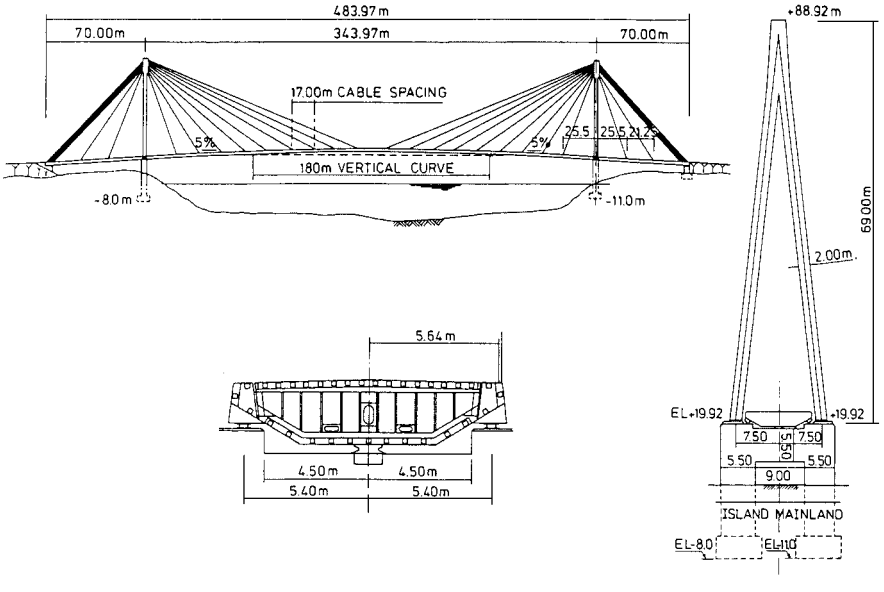

Figure 1. General characteristics of Jindo Bridge.

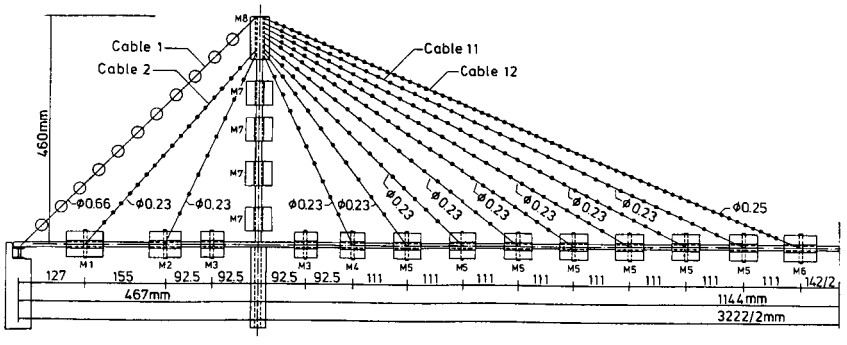

Figure 2. Overall characteristics and dimensions of the Jindo Bridge physical model.

The total length of the bridge model was 3.222 m, according to the linear scale factor $S_L = 150$. The choice of such a small scale was conditioned by the dimensions of the shaking table, and prevented the correct scaling of all aspects of the prototype. The box cross-sections of the girder and tower legs were substituted by solid rectangular cross-sections with correctly scaled bending stiffness (but not axial stiffness), maintaining the A-shape of the towers. These components, constructed in an aluminium alloy (Young's modulus $E_b = 72$ GPa), had the following dimensions: girder, 25.4×7.92 mm, tower legs, 9.2×8.4 mm. The stay cables were simulated with piano wires (Young's modulus $E_c = 210$ GPa). Their axial stiffness was correctly scaled and the only difference to the prototype was on the back stays, that were made of six cables in the real structure, and were constituted by one piano wire with equivalent scaled area in the model. To compensate for the dead weight of such a light model, additional masses were added. Small steel plates were attached to the towers and girders by two bolts, without any further contact to minimize any stiffening effects. Small lead spheres were glued along the cables that simulated the back stays. For the other cables, smaller masses made of a zinc alloy usually used as angling weights were attached to the cables simply by pressure. A general description of the overall bridge model can be found in Figure 2, while a more detailed characterization of the model is presented in Reference [3]. Table I summarizes the values of the scale factors used. Table II shows the characteristics of the added masses.

The set of final tensions on the cables from the bridge prototype was scaled according to the similitude theory, leading to the values of the prestress to be developed in the wires of the model, presented in Table III. This was achieved by turning bolts, around which the ends of the cables were wrapped, in the manner of tuning a violin. The tension in each cable was tuned indirectly using a magnetic sensor and a Fourier analyser, taking into account the relation between the natural frequencies of the cables and the corresponding tensions, according to the vibrating chord theory [19].

Table III summarizes the frequencies of the first three harmonics of the stay cables evaluated both on the basis of the Irvine theory [19], assuming a continuous idealization of the cables, and from a finite element formulation, dividing each cable into several truss elements with lumped masses at the nodes.

Table I. Scale factors of Jindo Bridge model.

Designation	Scale factor
Length	$S_L = 150$
Young's modulus (deck and towers)	$S_E^b = 3.07$
Young's modulus (cables)	$S_E^c = 0.748$
Mass (deck and towers)	$S_M^b = 3.07 \cdot (150)^2$
Mass (cables)	$S_M^c = 3.07 \cdot (150)^2$
Area (deck and towers)	$S_A^b = 150^2$
Area (cables)	$S_A^c = (3.07/0.748) \cdot (150)^2$
Inertia	$S_I^b = 150^4$
Force (deck, towers and cables)	$S_F^{b,c} = 3.07 \cdot (150)^2$
Time	$S_t = \sqrt{150}$
Frequency	$S_f = (150)^{-1/2}$

Table II. Characteristics of the added masses.

Location	Type of mass	Number of masses /cable	Total mass (kg)	Location	Type of mass	Total mass (kg)
Cable 1	Lead	11	0.306	Girder	Steel (M1)	1.83
Cable 2	Zinc	17	0.0267	Girder	Steel (M2)	1.63
Cable 3	Zinc	10	0.0157	Girder	Steel (M3)	1.20
Cable 4	Zinc	10	0.0157	Girder	Steel (M4)	1.31
Cable 5	Zinc	11	0.0173	Girder	Steel (M5)	1.45
Cable 6	Zinc	18	0.0283	Girder	Steel (M6)	1.68
Cable 7	Zinc	22	0.0348	Tower	Steel (M7)	2×0.4545
Cable 8	Zinc	32	0.0505	Tower	Steel (M8)	1.007
Cable 9	Zinc	35	0.0552			
Cable 10	Zinc	40	0.0631			
Cable 11	Zinc	44	0.0694			
Cable 12	Zinc	64	0.1009			

4. NUMERICAL EVALUATION OF MODAL PARAMETERS OF THE MODEL

Although it is recognized that the behaviour of cable-stayed bridges is clearly three dimensional and so a valid numerical analysis requires, in principle, a 3-D mathematical model, it was decided to develop, for simplicity in the first instance, a 2-D finite element analysis. The results obtained will not be reported in detail here but were used to prepare the experimental tests and to extract preliminary conclusions about the effect of the vibration of the cables on the global dynamic response of the bridge.

In a second phase, modal parameters were evaluated based on two 3-D finite element models of the Jindo Bridge physical model. These models were designated, according to Abdel-Ghaffar and Khalifa [15], as one-element cable system (OECS) and multi-element cable system (MECS) models. The OECS model discretized the deck and towers into 216 3-D beam elements (120, 80

Table III. Jindo Bridge model: natural frequencies of the stay cables.

Cable No.	Length (mm)	Mass (kg/m)	Tension (N)	1st Freq. (Hz) FEM (Irvine)	2nd Freq. (Hz) FEM (Irvine)	3rd Freq. (Hz) FEM (Irvine)
1	643.5	0.5258	123.1	11.46 (11.89)	22.61 (23.78)	33.42 (35.67)
2	513.0	0.05205	13.1	14.72 (15.46)	29.30 (30.93)	43.82 (46.39)
3	424.3	0.03724	9.6	17.90 (18.92)	35.46 (37.84)	52.35 (56.76)
4	424.4	0.03723	8.4	16.94 (17.70)	33.57 (35.39)	49.56 (53.09)
5	486.4	0.03577	8.0	14.64 (15.37)	29.06 (30.74)	43.00 (46.12)
6	558.7	0.05076	10.9	12.89 (13.11)	25.39 (26.23)	37.92 (39.34)
7	646.5	0.05375	12.0	11.22 (11.56)	22.40 (23.11)	33.53 (34.67)
8	740.7	0.06816	13.2	9.14 (9.39)	18.26 (18.79)	27.39 (28.18)
9	839.1	0.06581	14.8	8.95 (8.94)	17.44 (17.87)	26.15 (26.81)
10	940.3	0.06711	16.3	8.20 (8.29)	15.90 (16.57)	23.84 (24.86)
11	1043.6	0.06652	17.4	7.90 (7.75)	15.37 (15.50)	23.04 (23.25)
12	1148.4	0.08788	21.5	5.87 (6.81)	7.94 (13.62)	10.90 (20.43)

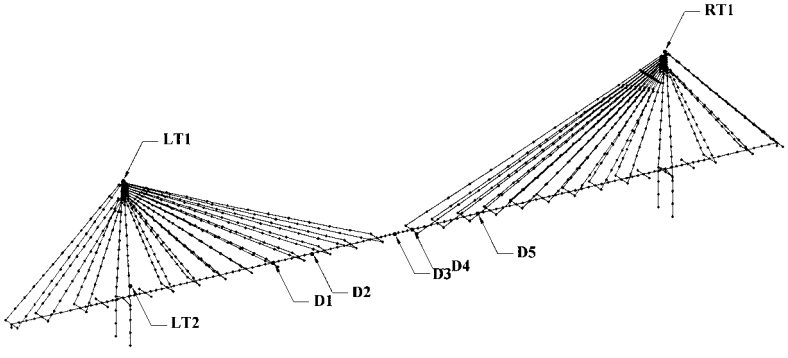

Figure 3. Structural discretization used in the MECS model.

and 16, for the deck, A-towers and piers, respectively) and idealized each stay cable as a simple truss element with an equivalent Young's modulus. Fifty six additional rigid link elements were added along the girder, in correspondence with added masses and cable end attachments (Figure 3). Forty eight additional elements of the same type were added at the top of the towers, in order to simulate the accurate length of the cables. Eleven additional stiff beam elements, connecting horizontally the two legs of each A-tower at the top, were also included, in order to obtain compatible displacements in conformance with the physical model. The MECS model adopted the same discretization of the deck and towers, and each stay cable was discretized into a total number of 12 truss elements.

The following boundary conditions were assumed in both models: (i) the piers were clamped to the soil; (ii) the vertical displacements, as well as the rotations around the longitudinal and vertical axes were precluded at the end supports of the deck; (iii) the transversal motion of the deck at the end and left tower supports was constrained by appropriate spring elements; (iv) additional constraints at the intermediate supports of the deck over the piers were introduced in

Table IV. Calculated natural frequencies of Jindo Bridge model (3-D OECS numerical model).

Mode number	Natural freq. (Hz)	Type of mode	Mode number	Natural freq. (Hz)	Type of mode
1	4.28	1st transversal SYM	11	24.95	1st torsion SYM
2	6.21	1st vertical SYM	12	26.00	3rd vertical ASM
3	9.12	1st vertical ASM	13	28.61	4th vertical SYM
4	11.71	1st transversal ASM	14	30.33	4th vertical ASM
5	13.74	2nd vertical SYM	15	30.45	transversal
6	18.26	2nd vertical ASM	16	30.46	5th vertical SYM
7	22.10	2nd transv.SYM + 1st torsion SYM	17	32.52	5th vertical ASM
8	22.70	3rd vertical SYM	18	38.80	2nd transv.ASM + 1st torsion ASM
9	23.42	1st LTW	19	39.69	6th vertical SYM
10	23.42	1st RTW	20	45.11	1st torsion ASM + 2nd transv. ASM

order to ensure compatibility of the deck and pier motions, imposing equal vertical displacements at the left support (Figure 3) and equal transversal and vertical displacements at the right one. The introduction of the design initial cable tensions was achieved iteratively by successive adjustment of the initial strain of the stay cables.

Using these models, dynamic analyses [20] were performed using the stiffness matrix obtained at the end of a geometric non-linear static analysis under permanent loads and a consistent mass matrix, which included in particular the rotational mass moments associated with the steel added masses along the deck and tower legs.

The lowest 20 natural frequencies in the range 0–46 Hz and the corresponding modal shapes were evaluated for the OECS. Table IV summarizes the values of these frequencies and the type of the corresponding modal shapes (SYM-mode shape of the girder and towers is approximately symmetric with respect to the axis of symmetry of the bridge; ASM-mode shape of the girder and towers is approximately anti-symmetric; LTW-mode shape involves essentially the movement of the left tower; RTW-mode shape involves essentially the movement of the right tower). For the MECS, the lowest 150 natural frequencies in the range 0–21.3 Hz and the corresponding modal shapes were calculated. Table V summarizes the values of some of these natural frequencies. It is worth mentioning that, for the first six modes obtained on the basis of the OECS model, there was no coupling between in-plane and out-of-plane motion, the first torsional mode occurring only at 22.1 Hz. Note that the non-existence of coupling between bending and torsion in terms of the first six natural frequencies led, in this case, to a significant proximity of the results provided by the 2-D and 3-D numerical models used to analyse the structural dynamic response. However, the value of 22.1 Hz is not really representative of the prototype torsional fundamental frequency, as the physical model did not respect the similarity requirements for the torsional behaviour.

Analysis of Tables IV and V and the observation of the modal shapes (see Figures 4 and 5) led to the conclusion that the MECS analysis, based on the discretization of the cables into several truss elements, produced many new modes of vibration. Most of the new modes simply involved local vibrations of the cables and so were not important in terms of the contribution to the global response of the bridge. Others of these new modes, however, involved simultaneous motion of the cables and of the deck and towers. In most cases, several of these modes of vibration had close

Table V. Calculated natural frequencies of Jindo Bridge Model (3-D MECS numerical model).

Mode number	MECS natural frequency (Hz)	Associated OECS frequency (Hz)	Ratio of participation factors (Z/Y)	Ratio of cable/beam max. displ (Z-ratio).	Ratio of cable/beam max. disp (Y-ratio).	Type of mode
1	4.26	4.28	< 1	532.1	**1.1**	1st transv. SYM
2	6.14	6.21	> 1	**1.0**	1066.4	1st vert. SYM
4	6.94	6.21	> 1	**6.1**	205509.8	1st vert. SYM
5	6.94	6.21	> 1	**5.8**	1845228.0	1st vert. SYM
9	7.15	11.71	< 1	77919.0	**3.3**	1st transv. ASM
10	7.16	4.28	< 1	83074.8	**16.2**	1st transv. SYM
12	7.93	9.12	> 1	**8.4**	148279.8	1st vert. ASM
13	7.93	9.12	> 1	**8.0**	2257478.0	1st vert. ASM
17	8.11	11.71	< 1	76110.7	**8.3**	1st transv. ASM
18	8.11	11.71	< 1	77946.7	**19.9**	1st transv. ASM
20	8.42	9.12	> 1	**3.8**	114344.9	1st vert. ASM
21	8.42	9.12	> 1	**3.7**	3830175.0	1st vert. ASM
25	8.61	11.71	< 1	69048.1	**3.2**	1st transv. ASM
26	8.61	11.71	< 1	65279.4	**17.3**	1st transv. ASM
27	9.04	9.12	> 1	**1.6**	2673.4	1st vert. ASM
29	9.63	9.12	> 1	**7.3**	77529.4	1st vert. ASM
30	9.63	9.12	> 1	**7.3**	9995453.0	1st vert. ASM
38	9.79	11.71	< 1	42457.2	**28.6**	1st transv. ASM
39	9.79	11.71	< 1	60449.4	**30.4**	1st transv. ASM
41	9.90	11.71	< 1	51944.1	**19.4**	1st transv. ASM
42	9.90	11.71	< 1	35404.6	**11.7**	1st transv. ASM
46	11.36	13.74	> 1	**5.8**	1065667.0	2nd vert. SYM
47	11.36	13.74	> 1	**6.4**	118704.9	2nd vert. SYM
48	11.45	13.74	> 1	**37.2**	29824.1	2nd vert. SYM
49	11.47	13.74	> 1	**35.2**	17452.5	1st vert. ASM
50	11.48	11.71	< 1	6395.6	**7.8**	1st transv. ASM
51	11.49	11.71	< 1	5927.5	**24.9**	1st transv. ASM
52	11.66	11.71	< 1	696.4	**11.3**	1st transv. ASM
55	12.00	13.74	> 1	**12.4**	248350.0	2nd vert. SYM
57	12.13	11.71	< 1	12735.4	**26.4**	1st transv. ASM
59	12.14	11.71	< 1	14815.6	**17.7**	1st transv. ASM
60	12.16	11.71	< 1	5180.5	**23.4**	1st transv. ASM
61	13.55	13.74	> 1	**6.4**	8786.0	2nd vert. SYM
63	13.75	13.74	> 1	**18.6**	795354.8	2nd vert. SYM
69	13.91	13.74	> 1	**35.3**	42291.0	2nd vert. SYM
77	14.12	13.74	> 1	**12.3**	19593.1	2nd vert. SYM

natural frequencies and similar mode shapes for the deck/towers system, but different movements of the cables, the relative order of magnitude of the motion also varying (see Figure 6). The analysis of the mode shapes showed that significant cable interaction occurred in a large number of modes, which could be subdivided into two groups. A first group was formed by modes of a vertical nature that presented a strong interaction in the vertical plane, associated with small ratios between the maximum vertical components of the normalized nodal displacements of the group of cables and of the deck/towers system (Z-ratio), though showing also in many cases large

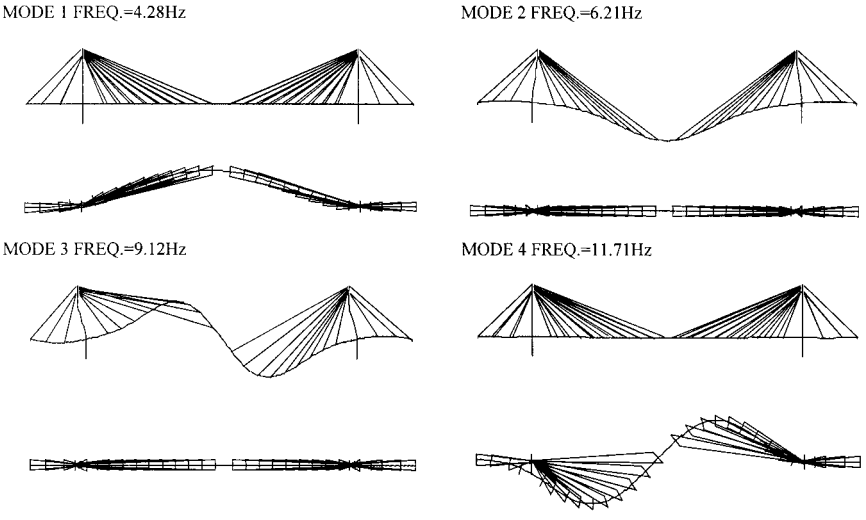

Figure 4. Some calculated modal shapes (OECS analysis).

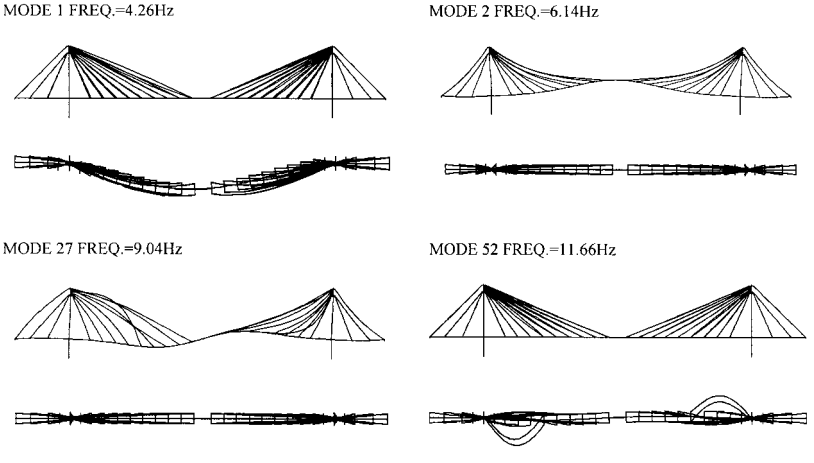

Figure 5. Some calculated modal shapes (MECS analysis).

out-of-plane cable displacements. A second group corresponded to transversal modes with a strong interaction for out-of-plane motions (small Y-ratios), though showing frequently large in-plane cable displacements. So, small values either of the Z-ratio or of the Y-ratio (indicated in bold type in Table V) denoted a very clear interaction between the cables and the girder/towers movement. High ratio values were typical of modal shapes that involved essentially vibration of one or more cables, here designated as local modes.

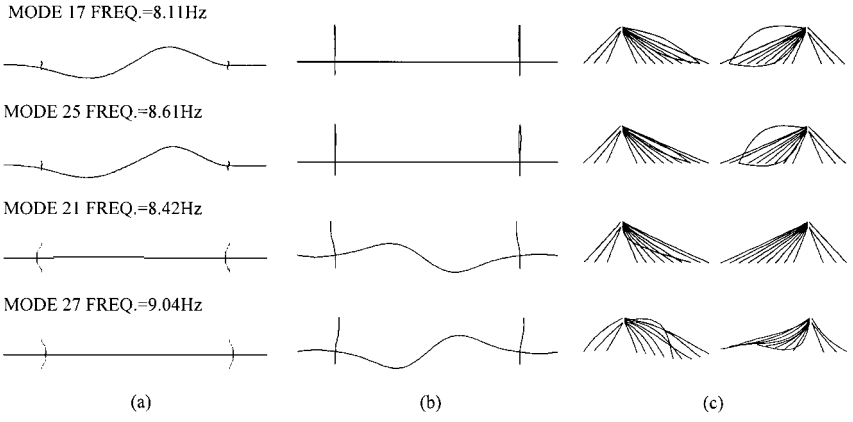

Figure 6. Some calculated modal shapes (MECS analysis): separated representation of cables and deck/towers motion (plan (a) and vertical views (b,c)).

5. EXPERIMENTAL MODAL SURVEY

5.1. Test procedures

The identification of modal parameters from the physical model was based on the use of an electrodynamic shaker. The procedure consisted of the application of vertical and transversal multi-sine excitation at the mid-span (node D3) and at the one third points of the span (left, node D2; right, node D5). The response was measured along the deck and towers using a small piezoelectric accelerometer, and along some of the cables, either using the piezoelectric accelerometer (only on the back-stays) or a magnetic sensor. Force was measured by means of a force sensor, interposed between the shaker and the bridge model.

The acquired time signals were used to obtain frequency response functions (FRFs). Modal parameters were extracted from the set of FRFs using a least-squares frequency-domain identification algorithm [21], based on the rational fraction polynomial method.

Figures 7 and 8 illustrate some examples of measured FRFs and associated coherence estimates for the range 0–100 Hz. The corresponding synthesized functions, based on the mentioned identification algorithm are also presented. Except for the range 0–10 Hz, where the noise-to-signal ratio is more significant, high coherence values were generally achieved, giving evidence of high-quality measurements.

Figure 9 presents some high quality FRF zooms performed in the low-frequency range, clearly showing the existence of several multiple vertical modes in the range 9–10 Hz.

Similar modal analysis tests were performed on a 6-DOF shaking table, by application of a multi-sine base excitation (along the longitudinal, X, transversal, Y, and vertical, Z, directions) and by measurement of the structural response in terms of accelerations and displacements along the deck and towers. Very good coherence function estimates were found in the range 0–50 Hz for the set of FRFs (obtained from the relation between the measured response and the measured acceleration on the shaking table) and, most important, there was high consistency between the

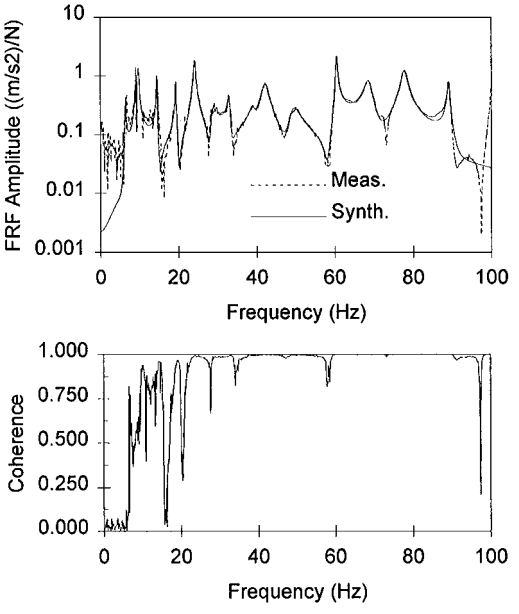

Figure 7. Coherence and FRF measured/synthesized from node D5 vertical (excitation) to node D1 vertical (response).

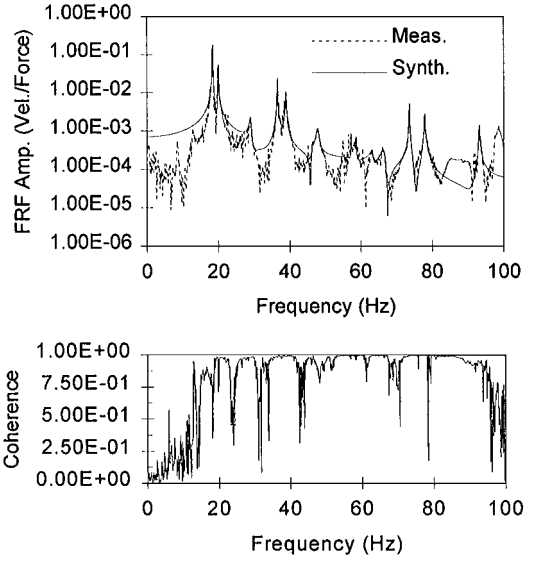

Figure 8. FRF and Coherence measured/synthesized from node D5 vertical (excitation) to cable 8 (left, back) between 10th and 11th masses from bottom (in-plane response).

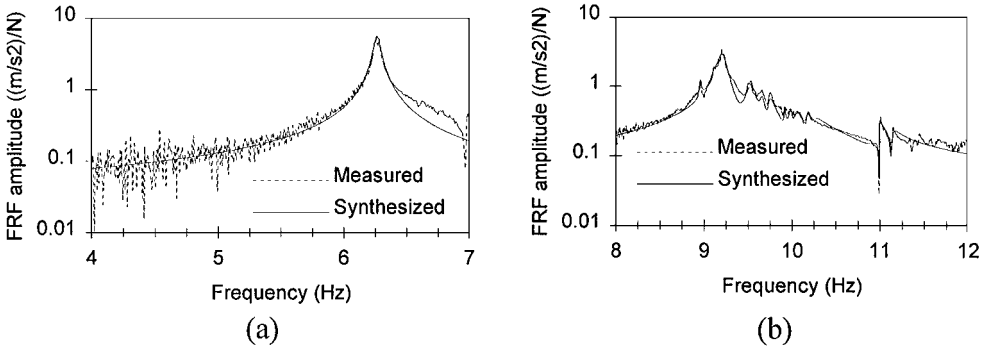

Figure 9. (a) Zoom FRF measured/synthesized from node D5 vertical (excitation) to node D3 vertical (response); (b) Zoom FRF measured/synthezised from node D5 vertical (excitation) to node D2 vertical (response).

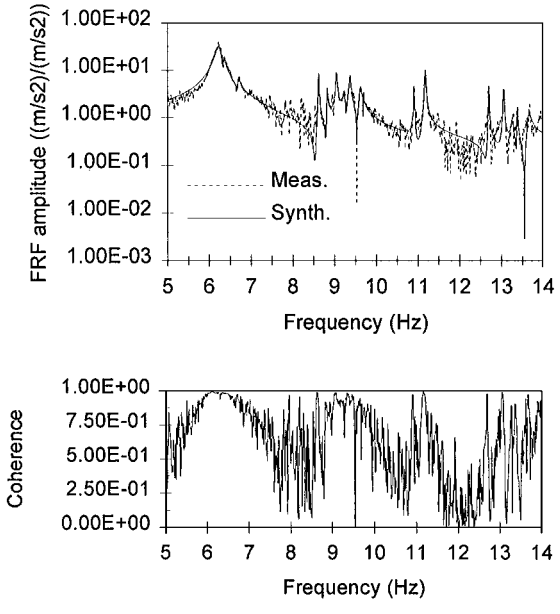

Figure 10. FRF and Coherence measured/synthesized from acceleration at the platform to node D5 vertical (response).

data obtained from these two different forms of excitation. Figure 10 presents an example of a measured/synthesized FRF and associated coherence function estimates.

5.2. *Test results*

Table VI summarizes the average values and the intervals of variation of the natural frequencies and damping factors, respectively, that were identified in the range 0–50 Hz. These were obtained

Table VI. Identified natural frequencies and damping factors.

Type of mode	Identified natural frequency (Hz)		Measured damping factor (%)	
	Shaker	Shaking table	Shaker	Shaking table
1st transv. SYM	3.95 ± 0.10	3.91 ± 0.09	—	1.65–2.08
1st vert. SYM	6.25 ± 0.08	6.27 ± 0.10	0.42–1.33	0.35–1.67
1st vert. SYM	6.69 ± 0.06	6.73 ± 0.03	0.60–0.87	0.11–0.43
1st vert. SYM	7.12 ± 0.06		0.52–0.91	
1st vert. ASM	8.96 ± 0.02	8.63 ± 0	0.13–0.16	0.060–0.069
1st vert. ASM		8.82 ± 0.01		0.092–0.097
1st vert. ASM	9.16 ± 0.06	9.05 ± 0.01	0.15–1.18	0.14–0.18
1st vert. ASM		9.25 ± 0.01		0.18–0.25
1st vert. ASM	9.52 ± 0.11	9.37 ± 0.06	0.15–0.78	0.19–0.25
1st vert. ASM	9.62 ± 0.09	9.49 ± 0.04	0.36–0.62	0.11–0.15
1st vert. ASM	9.74 ± 0.01	9.63 ± 0.03	0.19–0.22	0.15–0.29
1st vert. ASM	10.08 ± 0.16		0.14–0.30	
1st vert. ASM	11.00 ± 0.01	10.90 ± 0.02	0.15–0.17	0.043–0.049
1st vert. ASM	11.14 ± 0.01	11.18 ± 0.01	0.10–0.14	0.037–0.099
1st transv. ASM		9.10		0.34
1st transv. ASM		9.19		0.25
1st transv. ASM	9.62 ± 0		0.58–0.59	
1st transv. ASM	10.10 ± 0.08		0.60–0.90	
1st transv. ASM	10.27 ± 0.02	10.35 ± 0.11	0.28–0.30	0.52–1.73
1st transv. ASM	10.58 ± 0.06	10.54 ± 0.08	0.18–1.08	0.65–1.16
1st transv. ASM		10.73		0.60
1st transv. ASM	10.95 ± 0.01	10.98	0.08–0.12	0.094
1st transv. ASM	11.00 ± 0.03		0.10–0.33	
1st transv. ASM	11.18 ± 0.11	11.17 ± 0.03	0.03–0.82	0.81–1.13
1st transv. ASM	11.48 ± 0.03	11.49	0.02–0.25	0.12
1st transv. ASM	11.52 ± 0.01		0.21–0.32	
1st transv. ASM		11.62 ± 0.01		0.13–0.53
1st transv. ASM	11.88 ± 0.03		0.05–0.45	
1st transv. ASM		12.45		0.14
1st transv. ASM		12.66		0.11
1st transv. ASM		12.79		0.17
1st transv. ASM		12.82		0.61
1st transv. ASM		12.96		0.64
2nd vert. SYM	14.44 ± 0.12	14.36 ± 0.04	0.24–0.61	0.041–0.69
2nd vert. SYM	14.75 ± 0.09	14.51 ± 0.01		0.097–0.21
2nd vert. SYM		14.80 ± 0.02		0.16–0.24
2nd vert. ASM	18.74 ± 0.05		0.46–0.92	
2nd vert. ASM	19.05 ± 0.02	19.16 ± 0.08	0.16–0.25	0.039–0.47
2nd vert. ASM	19.23 ± 0.07	19.29 ± 0.09	0.14–1.09	0.16–0.41
2nd transv. SYM + 1st torsion SYM		20.24 ± 0.08		0.86–1.24
2nd transv. SYM + 1st torsion SYM		21.61 ± 0.03		0.07–0.32
2nd transv. SYM + 1st torsion SYM		21.97 ± 0.15		0.06–0.16
2nd transv. SYM + 1st torsion SYM		22.26 ± 0		0.01–0.28
2nd transv. SYM + 1st torsion SYM	23.24 ± 0.09	23.62 ± 0.17	0.14–0.47	0.038–0.098

Table VI. (continued)

Type of mode	Identified natural frequency (Hz)		Measured damping factor (%)	
	Shaker	Shaking table	Shaker	Shaking table
3rd vert. SYM	24.10 ± 0.33	23.89 ± 0.12		0.51–1.35
1st torsion SYM	25.19 ± 0.01			0.14–0.15
1st torsion SYM	25.49 ± 0.01			0.42–0.45
3rd vert. ASM	29.61 ± 0.67	27.59 ± 0.06	0.16–1.51	0.13–0.87
4th vert. SYM	30.48 ± 0.52	29.68 ± 0.56	0.24–1.80	0.33–1.88
4th vert. ASM	32.99 ± 0.12	33.42 ± 0.09	0.57–0.86	0.32–0.67
5th vert. SYM	39.33 ± 1.73	41.08 ± 0.53	0.96–2.06	0.63–1.22
5th vert. SYM	42.18 ± 1.58		0.87–2.29	
5th vert. ASM	49.35 ± 0.38		0.28–2.91	

from the set of FRF estimates associated with in-plane and out-of-plane excitation and response measurements, employing both types of excitation, electrodynamic shaker and shaking table tests.

Inspection of this table shows the consistency between measurements performed under excitation from the electrodynamic shaker and on the shaking table. Some slight differences obtained may be explained by perturbations induced by the shaker. In certain cases it was not possible to identify accurately some of the multiple modes simultaneously with both excitation techniques, due to high modal interference and insufficient amplitude and/or frequency resolution of the FRF estimates.

It is important to note the significant variation of the identified damping factors, which seem to be highly dependent on the amplitude of vibration and also on the duration of the excitation. This fact is particularly relevant for the damping factors associated to the first transversal and vertical bending modes of vibration, whose magnitudes also attained values much superior to other modes.

Table VII summarizes calculated natural frequencies based on the OECS and MECS models, as well as the corresponding average values of the identified natural frequencies, obtained from the shaking table measurements. These frequencies are grouped according to the deck/towers configuration of the associated mode shapes.

Inspection of the FRFs and of Tables VI and VII shows the existence of several very close natural frequencies in the vicinity of each of the natural frequencies obtained from the OECS analysis. This is probably due to the close proximity of the first natural frequencies of several cables with one of the natural frequencies of the global structure. This fact is more evident for the first transversal and vertical anti-symmetric modes obtained from the OECS analysis, as a significant number of modes have been identified. The FRF zoom presented in Figure 9(b), for instance, permitted the identification of nine vertical modes of vibration, at the frequencies 8.63, 8.83, 9.06, 9.24, 9.53, 9.62, 9.70, 10.92 and 11.18 Hz.

An attempt was made to prove that the measured mode shapes involved similar displacements for the girder and towers, and different displacements of the cables, as had been reported for the

Table VII. Identified and calculated natural frequencies.

Type of mode	OECS: Calculated natural frequency (Hz)	MECS: Calculated natural frequency (Hz)	Identified natural frequency (Hz)
1st transv. SYM	4.28	4.26/7.16	3.91
1st vert. SYM	6.21	6.14/6.94/6.94	6.27/6.73
1st vert. ASM	9.12	7.93/7.93/8.42/8.42/9.04/9.63/ 9.63/9.69/9.69/11.47	8.63/8.82/9.05/9.25/9.37/9.49 /9.63 /10.90/11.18
1st transv. ASM	11.71	7.15/8.11/8.11/8.61/8.61/9.79/ 9.79/9.90/9.90/11.48/11.49/11.66/ 12.13/12.14/12.16	9.10/9.19/10.35/10.54/10.73/ 10.98/11.17/11.49/11.62/12.45/ 12.66/12.79/12.82/12.96
2nd vert. SYM	13.74	11.36/11.36/11.45/11.47/12.00/ 12.00/13.55/13.75/13.75/13.91/ 14.12	14.36/14.51/14.80
2nd vert. ASM	18.26	17.81/18.29	19.16/19.29
2nd transv. SYM + 1st torsion SYM	22.10	*	20.24/21.61/21.97/22.26/23.62
3rd vert. SYM	22.70	*	23.89
1st torsion SYM	24.95	*	25.19/25.49

* Not calculated.

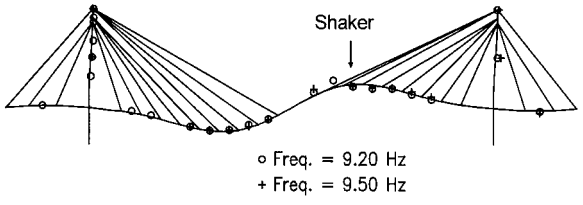

Figure 11. Identified and calculated mode shapes.

numerical analysis. Time series were collected at several nodes of the girder and towers, measuring the response to a sinusoidal excitation applied vertically at node D5 with frequencies of 9.20 and 9.50 Hz. From these series, components of the two mode shapes were estimated. Figure 11, representing a plot of these components against the associated values for the first vertical anti-symmetric mode obtained from the OECS analysis, shows the similarity of configurations of the mode shapes.

With regard to the cables, it was visually observed that sinusoidal excitations applied at closely spaced frequencies induced different movements of the cables. Moreover, for the levels of vibration induced, the persistence of the excitation showed no evidence of inducing a modification of the configurations of vibration (either of the girder/towers or of the cables) into other configurations (for instance, the configuration of adjacent modes of vibration). It was also

Table VIII. Observation of cable movement during sinusoidal excitation.

Frequency (Hz)	Cables connected to left tower	Cables connected to right tower
9.20	$\underline{8}D$, $\underline{\underline{8}}U$, $\underline{9}D$, $9U$, $\underline{3}U$	$\underline{\underline{8}}U$, $\underline{9}D$, $\underline{\underline{9}}U$, $\underline{5}D$, $\underline{5}U$
9.25	$\underline{8}D$, $\underline{\underline{8}}U$, $9D$, $9U$	$\underline{8}D$, $\underline{\underline{8}}U$, $\underline{9}D$, $\underline{\underline{9}}U$, $\underline{5}D$, $\underline{5}U$
9.50	$\underline{8}D$, $9D$, $9U$, $10D$, $10U$	$\underline{8}D$, $\underline{\underline{8}}U$, $\underline{9}D$, $\underline{\underline{9}}U$, $\underline{5}D$, $\underline{5}U$, $12D$, $12U$
9.55	$\underline{8}D$, $\underline{9}U$, $10D$, $10U$	$8U$, $9U$, $9D$, $\underline{5}D$

Table IX. Description of cable movement using a 3-D MECS analysis.

Frequency (Hz)	Cables connected to left tower	Cables connected to right tower
7.93	11	11
8.42	10	10
9.04	1, 7, $\underline{8}$, $\underline{9}$, 10, 11, 12	1, 7, $\underline{8}$, $\underline{9}$, 10, 11, 12
9.63	9	9
9.69	8	8
11.47	1	1

observed that the repetition of some sinusoidal excitations at different times and with different initial conditions did not induce different movements of the cables. Table VIII reports the observed movement of the cables for different frequencies of excitation close to 9 Hz. To distinguish the two cables connected to the upstream and downstream side of the same tower, symbols *D* (downstream cable) and *U* (upstream cable) have been employed. The relative amplitude of the cable movement is represented by i, $\underline{i}$ or $\underline{\underline{i}}$, the first meaning that the amplitude of vibration of cable i was low and the last meaning that this amplitude was quite high.

It is noteworthy that there was in fact a three-dimensional character of the vibration, as the four equal stay cables with similar tensions associated with each cable number (e.g.: 8U left, 8D left, 8U right, 8D right) behaved differently. From Tables VIII and IX, it is clear that the cables with major vibrations were the same in both experimental and numerical analyses. However, there was not a perfect agreement with the results of the 3-D MECS model in terms of the number and value of the identified frequencies or of the corresponding modal shapes. This fact is certainly due to the practical difficulty of achieving an accurate numerical model of local features and slight imperfections of the physical model.

With respect to the FRFs obtained from measurements on the cables, the analysis of peak frequencies revealed not only the frequencies of individual vibration of the cables, but also the existence of other peak values corresponding to natural frequencies measured on the girder/towers associated with global modes of vibration.

5.3. Accuracy of the analysis

The analysis presented in the previous sections used two different approaches (experimental and numerical) to determine the dynamic behaviour of a physical model of a cable-stayed bridge, which prompts some reflection about the corresponding accuracy and limitations.

With regard to the experimental analysis, two main sources of error can be identified: the errors associated with instrumentation and data acquisition, and the errors due to the algorithm used in the identification of structural parameters.

The instrument chain used in the shaker test had a 95 per cent confidence level calibration error of 5 per cent, leading to a maximum 10.6 per cent error in the amplitude of the FRF estimates. The chain calibrations for the instruments used in the shaking table tests were between 4 and 5 per cent, giving FRF amplitude errors between 8.3 and 9.1 per cent.

The relatively low level of these instrumentation errors, associated with the small-frequency resolution adopted (varying between 0.00625 and 0.1250 Hz) and the accurate identification algorithm used (a MDOF algorithm in the frequency domain that allows sub-interval curve-fitting and compensation of the effect of the out-of-band modes in manual mode), give confidence in the accuracy of the results.

With regard to the accuracy of the numerical modelling, it is worth noting that it faces some limitations and uncertainties. In fact, the numerical model could not take into account several physical features that can significantly influence the cable behaviour, for example, possible small imperfections in the connections of the cables to the girder and towers, lack of symmetry of the upstream and downstream cables due to the form of distribution of the added masses, as well as possible deviations of the cable tensions in relation to the theoretical values, due to the 5 per cent tolerance achieved in the cable tensioning. Moreover, some important uncertainties are also related with the constraints of the transversal motion of the deck at the end and left tower supports for transversal motions, and thermal changes are also disregarded.

6. FINAL CONSIDERATIONS

The main objective of this paper was to describe an experimental investigation developed by the authors at the Earthquake Engineering Research Centre of the University of Bristol, concerning the experimental study of the dynamic behaviour of the physical model of a cable-stayed bridge. From the set of data analysed, the following conclusions can be drawn:

1. Extensive measurements on the bridge model with associated high coherences showed good correlation with 3-D numerical models, suggesting a good quality of the database created.
2. The modal survey confirmed the existence of interaction between the cables and the deck/towers. This interaction was characterized by the appearance of several modes of vibration with very close natural frequencies and with similar mode shape configurations of the deck and towers, but involving different movements of the cables. The appearance of these new mode shapes proved to be conditioned by the closeness between a natural frequency of the global structure and the natural frequencies of some cables. Numerical analysis on the basis of the MECS model showed this aspect, although a perfect agreement between the calculated and the identified modal parameters could not be achieved, probably due to the practical difficulty of an accurate numerical modelling of local particularities and slight imperfections of the physical model.
3. The damping factors identified on the basis of both the modal survey and from the decay tests were in general rather small (less than 1 per cent) and exhibited a quite wide variation. This variation proved to be related to the amplitude of motion and to the duration of

excitation, and was more significant for the first vertical and transversal bending modes of vibration.

ACKNOWLEDGEMENTS

The present investigation work was carried out at the EERC at the University of Bristol and funded from the Human Capital and Mobility Programme of the European Union, under the ECOEST Programme (European Consortium of Earthquake Shaking Tables) and in conjunction with research contracts from the UK Engineering and Physical Sciences Research Council and from the Portuguese Foundation for Science and Technology (FCT). The writers wish to acknowledge the help of Prof. R. Severn who provided material conditions for this research, as well as the advice of Dr A. Blakeborough and the technical support of Mr D. Ward.

REFERENCES

1. Sethia MR, Krishna P. Modal tests of a cable-stayed bridge. *Proceeding of the International Conference on Cable-Stayed Bridges*, Bangkok, 1987; 927–938.
2. Godden WG, Aslam, M. Dynamic model studies of a Ruck-A-Churcky bridge. *Journal of the Structural Division*, ASCE, 1978; **104**(ST12):1827–1844.
3. Garevski MA. Dynamic analysis of cable-stayed bridges by means of analytical and physical modelling. *Ph.D. Thesis*, Department of Civil Engineering, University of Bristol, U.K., 1990.
4. Stiemer SF, Taylor P, Vincent DHC. Full scale dynamic testing of the Annacis bridge. IABSE Periodica, 1988; **1**:1–16.
5. Ohlsson SV. Dynamic characteristics of cable-stayed bridges—nonlinearities and weakly coupled modes of vibration. *Proceedings of the International Conference on Cable-Stayed Bridges*, Bangkok, 1987; 421–431.
6. Murià-Vila D, Gomèz R, King C. Dynamic structural properties of cable-stayed Tampico Bridge. *Journal of structural engineering*, ASCE, 1991; **117**(11):3396–3416.
7. Jakobsen KA, Jordet E, Rambjor SK, Jakobsen AA. Full scale measurements of the behaviour of the Helgeland bridge—a cable-stayed bridge located in a harsh environment. *Proceedings of the International Symposium on Cable Dynamics*, Liège, 1995; 473–480.
8. Cremer J-M, Counasse C, Goyet VV, Lothaire A, Dumortier A. The stays, their dynamic behaviour, their equipments—Bridges at Ben-Ahin, Wandre and upon Alzette. *Proceedings of the International Symposium on Cable Dynamics*, Liège, 1995; 489–496.
9. Langsoe HE, Larsen OD. Generating mechanisms for cable stay oscillations at the Faro bridges. *Proceedings of the International Conference on Cable-Stayed Bridges*, Bangkok, 1987; 1023–1033.
10. Persoon AJ. The wind induced response of a cable-stayed bridge. *Bridge Aerodynamics*, Proc. of ICE Conf., 1981; 73–77.
11. Lilien JL, Costa AP. Amplitudes caused by parametric excitations on cable stayed structures. *Journal of Sound and Vibration*, 1994; **174**(1):64–90.
12. Hikami Y, Shiraishi N. Rain-wind induced vibrations of cables in cable-stayed bridges. *Journal of Wind Engineering and Industrial Aerodynamics*, 1988; **29**:409–418.
13. Ruscheweyh H, Verwieke C. Rain-wind-induced vibrations of steel bars. *Proceedings of the International Conference on Cable-Stayed Bridges*, Bangkok, 1987; 469–472.
14. Causevic MS, Sreckovic G. Modelling of cable-stayed bridge cables: effects on bridge vibrations. *Proceedings of the International Conference on Cable-Stayed Bridges*, Bangkok, 1987; 407–420.
15. Abdel-Ghaffar AM, Khalifa MA. Importance of cable vibration in dynamics of cable-stayed bridges. *Journal of Engineering Mechanics*, ASCE, 1990; **117**(11):2571–2589.
16. Caetano E, Cunha A, Taylor CA. Investigation of dynamic cable-deck interaction in a physical model of a cable-stayed bridge. Part II: seismic response. *Earthquake Engineering and Structural Dynamics*, 1999, accepted.
17. Tappin GR. Jindo and Dolson Bridges. *Proceedings of the Institute of Civil Engineers*, 1985; **78**(Part I):1281–1300.
18. Caetano E, Cunha A. An investigation into the cable dynamics on cable-stayed bridges. *Research Report*, Department of Civil Engineering, University of Bristol, U.K., 1995.
19. Irvine HM. Vibrations of inclined cables. *Journal of Structural Division*, ASCE, 1978; **104**(ST2):343–347.
20. SOLVIA 95.0 Finite element system, SOLVIA Engineering AB, Sweden, 1995.
21. Han M-C, Wicks AL. On the application of Forsythe orthogonal polynomials for global modal parameter estimation. *Proceedings of the 7th International Modal Analysis Conference*, 1989; 625–630.

